Mathematical Biosciences and Engineering

https://www.aimspress.com/journal/mbe

MBE, 21(4): 5164–5180.
DOI: 10.3934/mbe.2024228
Received: 03 February 2024
Revised: 27 February 2024
Accepted: 29 February 2024
Published: 05 March 2024

Research article

The impact of MCCK1, an inhibitor of IKBKE kinase, on acute B lymphocyte leukemia cells

Shuangshuang Wen[1], Peng Zhao[2], Siyu Chen[3], Bo Deng[1], Qin Fang[4] and Jishi Wang[2,*]

[1] Guizhou Medical University, Guiyang 550004, China
[2] Hematology Department, Affiliated Hospital of Guizhou Medical University, Guiyang 550004, China
[3] The Second Affiliated Hospital, The Third Military Medical University, Chongqing 400000, China
[4] Pharmacy Department, Affiliated Hospital of Guizhou Medical University, Guiyang 550004, China

* **Correspondence:** Email: wangjishi123456@163.com.

Abstract: B-cell acute lymphoblastic leukemia (B-ALL) is a malignant blood disorder, particularly detrimental to children and adolescents, with recurrent or unresponsive cases contributing significantly to cancer-associated fatalities. IKBKE, associated with innate immunity, tumor promotion, and drug resistance, remains poorly understood in the context of B-ALL. Thus, this research aimed to explore the impact of the IKBKE inhibitor MCCK1 on B-ALL cells. The study encompassed diverse experiments, including clinical samples, in vitro and in vivo investigations. Quantitative real-time fluorescence PCR and protein blotting revealed heightened IKBKE mRNA and protein expression in B-ALL patients. Subsequent in vitro experiments with B-ALL cell lines demonstrated that MCCK1 treatment resulted in reduced cell viability and survival rates, with flow cytometry indicating cell cycle arrest. In vivo experiments using B-ALL mouse tumor models substantiated MCCK1's efficacy in impeding tumor proliferation. These findings collectively suggest that IKBKE, found to be elevated in B-ALL patients, may serve as a promising drug target, with MCCK1 demonstrating potential for inducing apoptosis in B-ALL cells both in vitro and in vivo.

Keywords: acute lymphocytic leukemia; IKBKE kinase; MCCK1; apoptosis

1. Introduction

Acute lymphoblastic leukemia (ALL) is an acute form of lymphoblastic leukemia or lymphoma characterized by a variety of genetic mutations in individuals with a typical chromosomal structure in traditional cytogenetics. Approximately 25% of childhood cancers are attributed to this malady, and adults can also be afflicted with it [1, 2]. The primary treatment for ALL is multidrug chemotherapy,

such as the VP regimen (Vincristine and Dexamethasone) and others. Despite generally successful results, approximately 20% of B-ALL patients become resistant to treatment during their therapy [3]. Furthermore, recurrent chromosomal abnormalities are common in B-ALL, leading to a high rate of relapse [4, 5]. For individuals with R/R ALL, the search for more effective treatments and medications is urgent. In the past, chemotherapy drugs have been the primary treatment for R/R ALL. However, CRR (complete remission rates) for first- and second-line treatments are only 30 to 40% and 10 to 20%, respectively [6]. Despite the emergence of various new treatments, the prognosis of patients with recurrent or refractory diseases is still severe, and patients with a survival time of more than five years are still less than 10% [7]. Moreover, research has demonstrated that the persistence of minuscule amounts of disease (MRD) following induction treatment may be linked to unfavorable outcomes [8], such as a greater risk of relapse and a shorter lifespan [9]. Consequently, it is essential to investigate novel therapies to enhance patient well-being and stimulate scientific inquiry.

IKBKE (molecular weight 80 KD) is a non-classical protein of IKK (IκB kinase) and has an essential role in immune signaling, phagocyte activation, and a variety of metabolic disorders [10, 11]. The expression of IKBKE has been associated with a pivotal regulatory role in the growth and advancement of a range of malignant tumors, including Kaposi's sarcoma, ovarian cancer, gastric cancer, and glioma, and is often highly expressed in other solid tumors [12–14]. Research conducted both in vitro and in vivo has proven that a decrease in IKBKE expression has a significant impact on the hyperplasia of multiple cancer cells, causes the cells to die more quickly, and decreases the cells' ability to invade and move [15]. Studies conducted in the past have demonstrated that IKBKE is present in some types of blood cancers, such as AML, Burkitt's lymphoma, diffuse large B-cell lymphoma, B-ALL, T-ALL, and multiple myeloma [16–18]. Some scholars have found that IKBKE manages the development of multiple types of cancer [19], as well as contributing to tumor growth, cell invasion, and resistance to drug treatments [20]. However, the role and related mechanisms in which IKBKE operates in B-ALL have yet to be determined. Therefore, the purpose of this study is to explore the effect of IKBKE in B-ALL and identify new targets for clinical treatment.

MCCK1 is a malachite green oxalate compound that is particularly effective at inhibiting IKBKE and its associated pathways (Figure 2A) [21, 22]. Liu et al. [23] found that MCCK1 can enhance the anticancer effect of temozolomide on the invasion, migration, and epithelial-mesenchymal transition of solid tumor cells in vitro and in vivo. Another study has demonstrated that MCCK1 can selectively combat IKBKE both in vitro and in vivo, but the effect of MCCK1 on B-ALL has yet to be determined. Therefore, this research demonstrates the high expression level of IKBKE in B-ALL patients and assesses its influence on cell proliferation, division, and B-ALL-derived tumors both in vitro and in vivo.

2. Materials and methods

2.1. Patients and specimen

Bone marrow samples were extracted for IKBKE expression analysis in 35 patients with an initial B-ALL diagnosis obtained from the Affiliated Hospital of Guizhou Medical University (Table 1). Ficoll gradient centrifugation was utilized to separate mononuclear cells from bone marrow [24]. The WHO 2021 criteria were used to determine B-ALL. The Institutional Review Board of the Affiliated Hospital of Guizhou Medical University authorized the research project, and all participants were made aware

of their rights as outlined in the Declaration of Helsinki before granting their consent.

Table 1. Patients' characteristics.

	Descriptive statistics
Total patients	35
Median age, years (min-max)	29 (5–66)
Age	
<10	4 (11.4%)
10–40	21 (60.0%)
>40	10 (28.6%)
White blood cells count ($\times 10^9$/L)	
<10	8 (22.9%)
10–99	16 (45.7%)
>=100	11 (31.4%)
Cytogenetics	
Ph (+)	12 (34.3%)
IGH (+)	4 (11.4%)
Normal	19 (54.3%)
Immunophenotype	
Pro-B-ALL	8 (22.9%)
Pre-B-All	5 (14.3%)
Common-B-All	22 (62.8%)

2.2. Cells lines and culture

Human B-ALL cell lines NALM-6 and RS4:11 were extracted from the Guizhou Province Hematopoietic Stem Cell Transplantation Center to be utilized in cell culture and cultivated in RPMI-1640 medium or DMEM medium (Tianhang Biotechnology Co., Ltd., Hangzhou, China) supplemented with 10% fetal bovine serum and 1% penicillin/streptomycin (Cyagen Biosciences, Guangzhou, China) in a 37°C/5% CO2 environment.

2.3. Quantitative reverse transcriptase-polymerase chain reaction (qRT-PCR)

The reagents were employed: MCCK1, the specific selective IKBKE inhibitor (MedChemExpress, USA); reverse transcription kit (Thermo, USA); PBS solution (Hyclone, USA); fetal bovine serum (Ex-Cell Bio, China); RPMi-1640 medium (gibco BRL); fetal bovine serum (Tianhang Biotechnology Co., Ltd., Hangzhou, China); 0.25% trypsin-0.02% EDTA (Tianhang Biotechnology Co., Ltd., Hangzhou, China); Cell Counting Kit-8 (7Sea Biotech, Shanghai, China); and Matrix gel (Corning, USA).

2.4. Reagents and antibodies

The cell samples were collected, mixed with 1 ml of Trizol, and centrifuged to obtain a colorless supernatant, then mRNA was extracted by adding isopropanol and ethanol, and the concentration was measured for evaluation. The mRNA was reverse transcribed using the reverse

transcription kit to obtain cDNA (reaction conditions: 42°C for 15 min; 95°C for 3 min). Finally, the cDNA was quantified in real time using Real Master Mix (SYBR Green) (Tiangen Biochemical Technology Co., Ltd., Beijing) and target primers according to the manufacturer's instructions (reaction conditions: 95°C:3 minutes,1cycle; 95°C:5 seconds and 60°C:1 minute for 40 cycle). β-actin was selected as an internal standard to assess mRNA levels. The following are the specific sequences of the primers utilized in the PCR process: IKBKEF:5'-GGACCCACAGGAAAGAGTG-3'; IKBKER:5'-GGGAAGGCGTATGAGAGC-3'; β-actinF:5'-CTACCTCATGAAAGATCCTCACCGA-3'; β-actinR:5'-TTCTCCTTAATGTCACGCACGATT-3'.

2.5. Western blot analysis

The erythrocyte lysate was added to the bone marrow blood, shaken rapidly for 5 min, then centrifuged at 1500 rpm for 5 min, and the supernatant was discarded. The cell precipitate was then washed with cold PBS. PMSF (Sigma, China) and RIPA lysate were then added at a ratio of VPMSF: VRIPA=1:99, the supernatant (4°C) was centrifuged after thorough mixing, and after a series of reactions and thermal denaturation, the protein samples were extracted by adding SDS-PAGE protein loading buffer (Solabio, Beijing). The proteins were electrophoresed, transferred to polyvinylidene fluoride membranes, and immobilized in a mixture of PBS and 5% skim milk powder. The membranes were then cryoprotected for 2–4 hours and then rinsed. The primary antibody is incubated with the membrane for 2 hours. Once complete, the membranes are washed and then immersed for 45 minutes at room temperature in a secondary antibody solution from Protein Biotechnology. Lastly, using A and B liquids (7SeaBiotech), color development was used to show the protein spectrum.

2.6. Cell counting kit-8 (CCK-8) proliferation assay

The CCK-8 assay was employed to evaluate the cell's survival capability following MCCK1 treatment. The B-ALL cells were preplaced on 96-well plates with 6 sub-wells per group at a density of 5000–10,000 cells per well. Following the experimental methodology, various drug concentrations were introduced, making sure that each well had a total volume of 200 μl. Each well should contain 20 μl of CCK reagent. After gently mixing and another 30–120 minutes in the incubator, measure the absorbance at 450 nm with a spectrophotometer. (Molecular Devices, Sunnyvale, CA, USA).

2.7. Apoptosis analysis was performed using membrane-linked protein V-FITC/propidium iodide (PI) labeling

Following incubation, cell suspensions from various wells were aspirated into flow-through tubes and centrifuged at 1000 rpm for 5 min before being washed and centrifuged once more. 3.5 μL of Annexin V-FITC (7Sea Biotech) and 5 μL of PI (7Sea Biotech) staining solution were mixed completely, added to the flow tube with cell precipitation, and incubated for 15 minutes at room temperature. A flow cytometer was then used to check for apoptosis. Quantitative analysis: To analyze the data and determine the percentage of apoptotic cells, Flow Jo software was used.

2.8. Cell cycle analysis

Cells were treated following the experimental plan, collected, processed, and heated to 37°C for 30 minutes in the dark before being left in the dark. A BD Biosciences FACSCalibur flow cytometer

and Multicycle software were used for detection and analysis. According to the protocol, the cells were plated and given a pharmacological treatment for 24 hours. The cells were then fixed in 70% pre-cooled ethanol overnight at 4°C. The cell cycle stage of these samples was then determined using FACScan flow cytometry.

2.9. In vivo experiment

Female NOD/SCID mice, aged four to six weeks, were obtained from SPF Biotechnology (China Ltd.). These mice are non-obese and severely immunodeficient. We mixed Matrigel (Corning, USA) with Nalm-6 cells (1×10^7) and implanted the mixture into the left abdomen of the mice. We randomly assigned all mice to two groups: one group received vehicle (saline) and the other group received 10 mg/kg MCCK1 (every other day) [11]. Tumor volume changes were recorded (tumor volume (mm3) was computed as $(L \times W^2)/2$, where L is the maximum diameter of the tumor and W is the minimum diameter of the tumor), and measurements were performed twice a week [25]. The ethics committee of Guizhou Medical University approved all animal experiments used in this study.

2.10. Histopathological analysis of tumors

After the xenograft tumors were removed, they were promptly preserved in 4% paraformaldehyde. Next, they were embedded in paraffin wax and sliced into pieces of around 3 μm. To observe cell characteristics, H&E staining was utilized, and the samples were viewed under a light microscope. To evaluate apoptosis in situ, we utilized the TUNEL Apoptosis Detection Kit (Beyotime) and performed the terminal dUTP nick-labeling assay (TUNEL) to check DNA fragmentation in the nucleus. The proportion of apoptotic cells was determined by observing sections under a fluorescent microscope.

2.11. Statistical analysis

GraphPad Software 8.0 (GraphPad Software, CA, USA) was employed to conduct statistical analyses. The quantitative data, which followed a normal distribution, was expressed using the mean ± SD method, and the means of different samples were compared using t-tests or ANOVA tests. Unless otherwise stated, the data are the mean and standard deviation of three independent experiments. $p < 0.05$ represents statistical significance.

3. Results

3.1. Expression level of IKBKE in B-ALL patients

The IKBKE kinase is recognized for its high expression in various types of cancer. Recent studies have revealed increased expression in both hematological and solid tumors [26, 27]. This research examined the expression level of IKBKE in BM-MNCs taken from people with B-ALL patients and controls using RT-PCR (Figure 1A). Accordingly, IKBKE expression was significantly higher in B-ALL patients than in healthy control subjects ($p < 0.0001$). Additionally, Western blotting also demonstrated heightened IKBKE protein levels in B-ALL individuals (Figure 1B,C).

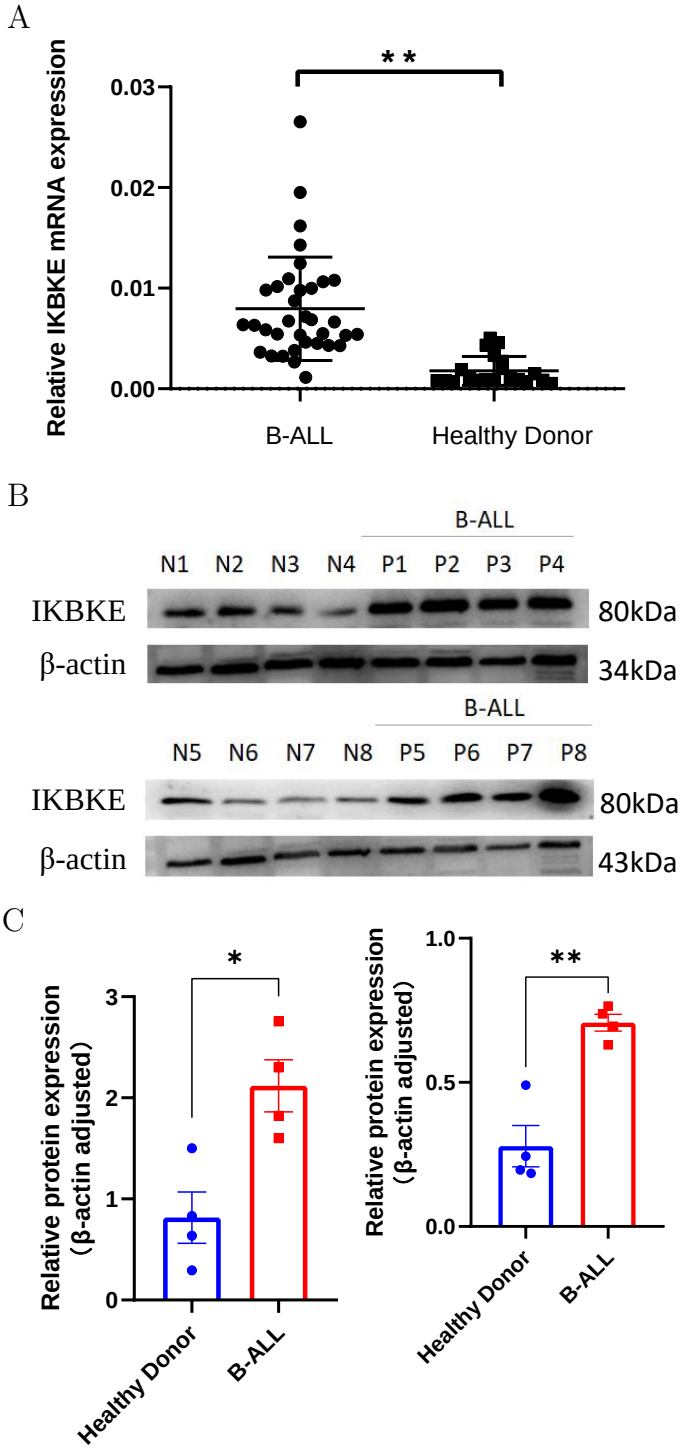

Figure 1. The expression level of IKBKE in B-ALL patients. (A) Real-time PCR was used to analyze the mRNA expression of IKBKE in BM-MNC from B-ALL patients (n = 35). Data are expressed as mean ± standard deviation; *, $p < 0.05$ compared to healthy controls; **, $p < 0.01$ compared to healthy controls. (B) IKBKE protein levels in B-ALL samples were measured by protein blotting. Loading control, β-actin. (C) Protein blot results between the two groups were compared by grayscale analysis. Variances were statistically significant compared to controls: *, $p < 0.05$, and **, $p < 0.01$.

3.2. MCCK1 inhibits the growth of B-ALL cells in vitro

Despite evidence that the IKBKE kinase inhibitor MCCK1 has the capacity to prevent the proliferation of various solid tumor cells, there has yet to be any research done to assess the impact of MCCK1 on leukemia cells, particularly B-ALL cell lines. In order to investigate clinical treatment strategies, we exposed two cell lines, NALM-6 and RS4:11 B-ALL, to varying concentrations of IKBKE for 24 and 48 hours, respectively. We then measured their viability using the CCK-8 assay. After being treated with IKBKE, the viability of both B-ALL cell lines (NALM-6 and RS4:11) was inhibited in a significant dose- and time-dependent manner (Figure 2B, $p < 0.01$). At the same time, the cell viability of NALM-6 and RS4:11 was higher after 24 hours of MCCK1 treatment than after 48 hours of MCCK1 treatment. In addition, the NALM-6 cells were found to be more responsive to MCCK1 than RS4:11 cells, with an IC50 of 6.365 μM and 6.747 μM, respectively (Figure 2C).

3.3. MCCK1 affects apoptosis and the cell cycle of B-ALL cells

This study examined the effects of MCCK1 on B-ALL cell proliferation for the first time by looking into the drug's potential to control apoptosis. The research revealed that the number of apoptotic cells increased in proportion to the concentration of MCCK1 following treatment (Figure 3A). In NALM-6 cells, the apoptosis rate increased to 41.02% after treatment with 5 μM MCCK1, whereas in RS4:11 cells, the rate was lower at 35.18% (Figure 3B).

Altered cell cycle progression is a known cause of apoptosis. Previous studies have found that downregulation of IKBKE can induce apoptosis of malignant tumor cells and result in cell cycle arrest in the G0/G1 phase [28]. However, as of yet, no studies have identified a correlation between MCCK1 and the B-ALL cell cycle. The aim of this study was to investigate the impact of MCCK1 on the B-ALL cell cycle. The results obtained through flow cytometry indicated that MCCK1 caused cell blockage in the G0/G1 phase (Figure 3C). Specifically, treatment with 4 μM MCCK1 resulted in a significant increase in the number of NALM-6 cells in the G0/G1 phase, from 9.98 to 51.07%, and the ratio of RS4:11 cells in the same phase increased from 33.95 to 52.26% (Figure 3D).

3.4. The impact of MCCK1 on the growth of tumor in vivo

To examine the impact of MCCK1 on tumor growth in vivo, we injected NALM-6 cells (known to be more responsive to MCCK1) beneath the skin of NOD/SCID mice. Treatment with MCCK1 was initiated on day 12 (once the tumors were palpable). This treatment was administered every other day until the 45th day (Figure 4A). Treatment with MCCK1 significantly inhibited the growth of NALM-6 cell-derived tumors (Figure 4B,C). The MCCK1-treated mice with transplanted tumors exhibited an extended overall survival time compared to the control mice, which had a shorter overall survival (Figure 4D). The H&E staining of xenograft tumors reveals a disorganized arrangement of tumor cells and an increase in nucleoplasmic content, which is indicative of malignancy (Figure 4E). TUNEL fluorescence analysis revealed that there were more apoptotic cells in the MCCK1-treated group than in the saline-treated group (Figure 4F,G).

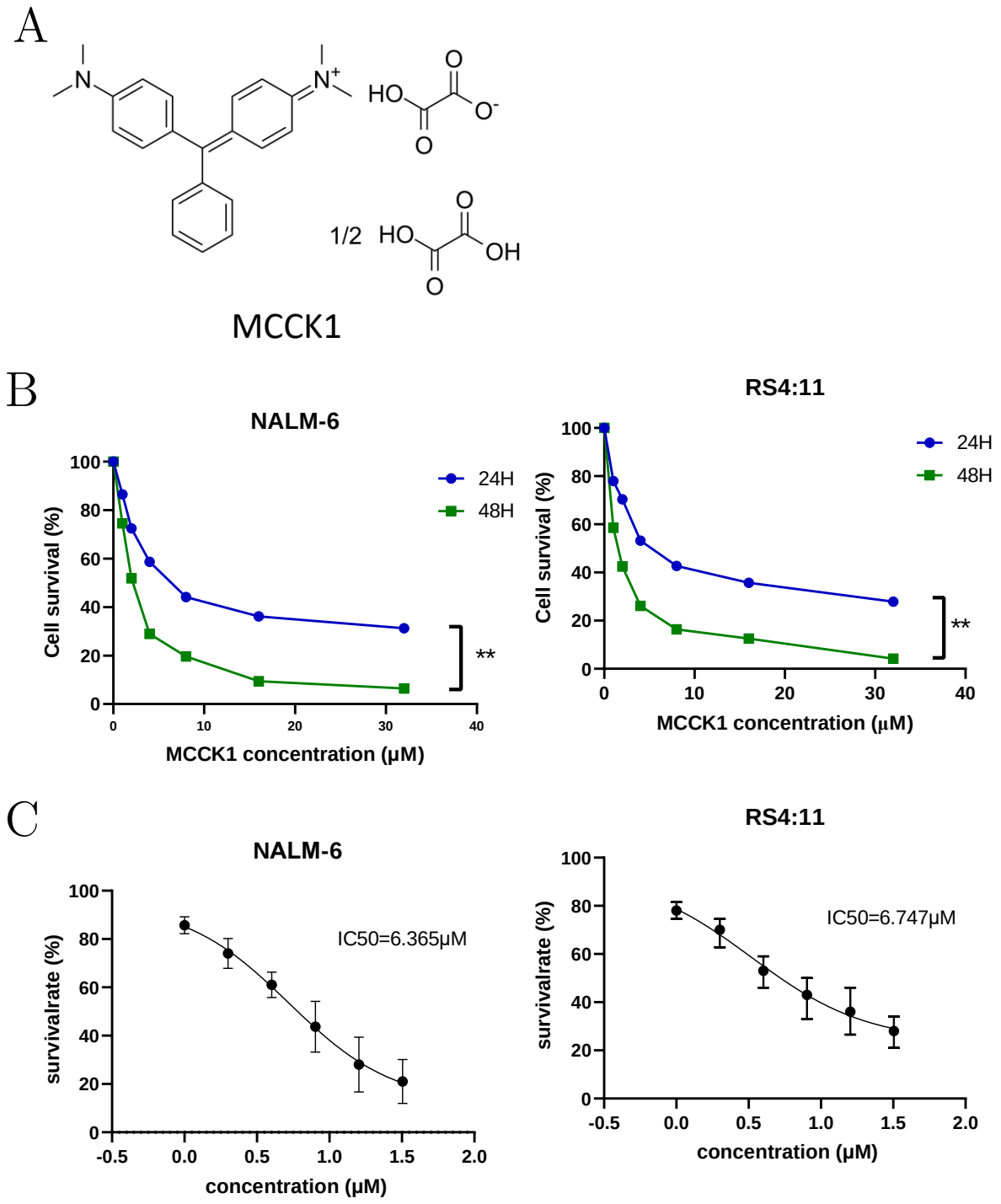

Figure 2. Inhibition of B-ALL cell growth by MCCK1 in vitro. (A) The structure of MCCK1. (B) The viability of Nalm-6 and RS4:11 cells were assessed using the CCK-8 assay after being exposed to concentrations of 0, 1, 2, 4, 8, 16, and 32 μM MCCK1 for 24 and 48 hours, respectively. (C) Cells were exposed to a range of concentrations of MCCK1 from 0 to 32 μM over a 24-hour period, and the results were measured with the CCK-8 assay. IC50 values were determined by using GraphPad 8.0 software. Data are expressed as mean ± standard deviation; *, $p < 0.05$ compared to the 0 μM group; **, $p < 0.01$ compared to the 0 μM group.

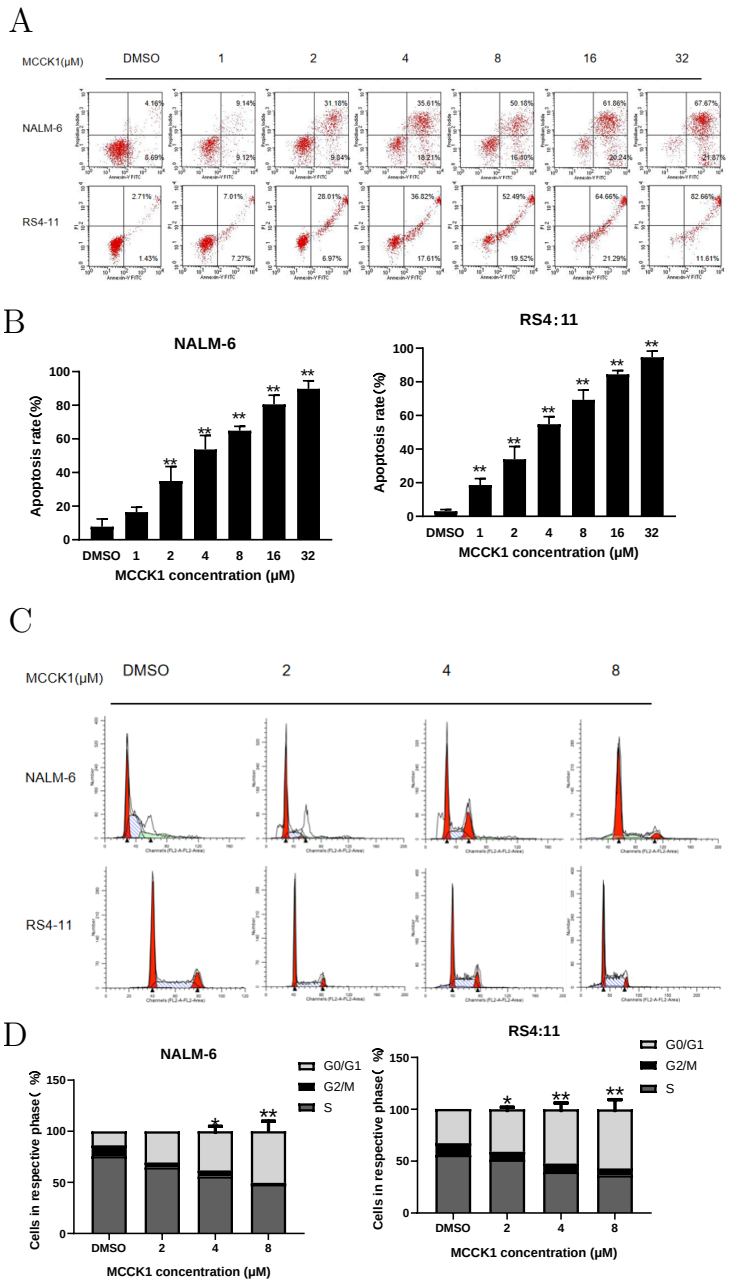

Figure 3. MCCK1 has been found to induce apoptosis in B-ALL cells, resulting in the accumulation of these cells in the G0/G1 phase. (A) The effects of MCCK1 (0, 1, 2, 4, 8, 16, and 32 μM) on NALM-6 and RS4:11 cells were evaluated after 24 hours by measuring apoptosis rates through V-FITC/PI staining of cell membrane proteins. The data presented in this paper is the result of integrating information from three separate experiments. (B) The three experiments examined the apoptosis rates of NALM-6 and RS4:11 cells. Data are shown as mean ± standard deviation; *, $p < 0.05$ compared to the DMSO group; and **, $p < 0.01$ compared to the DMSO group. (C) After treating NALM-6 and RS4:11 cells with concentrations of 0, 2, 4, and 8 μM MCCK1 for 24 hours, a flow cytometric analysis was conducted, and the cells were stained with a solution that contained PI, Rnase A, and staining buffer. These images illustrate the cell cycle distribution of B-ALL cells. (D) The proportion of cells in each phase of the cell cycle. Data are expressed as mean μ standard deviation; *, $p < 0.05$ compared to the DMSO group; **, $p < 0.01$ compared to the DMSO group.

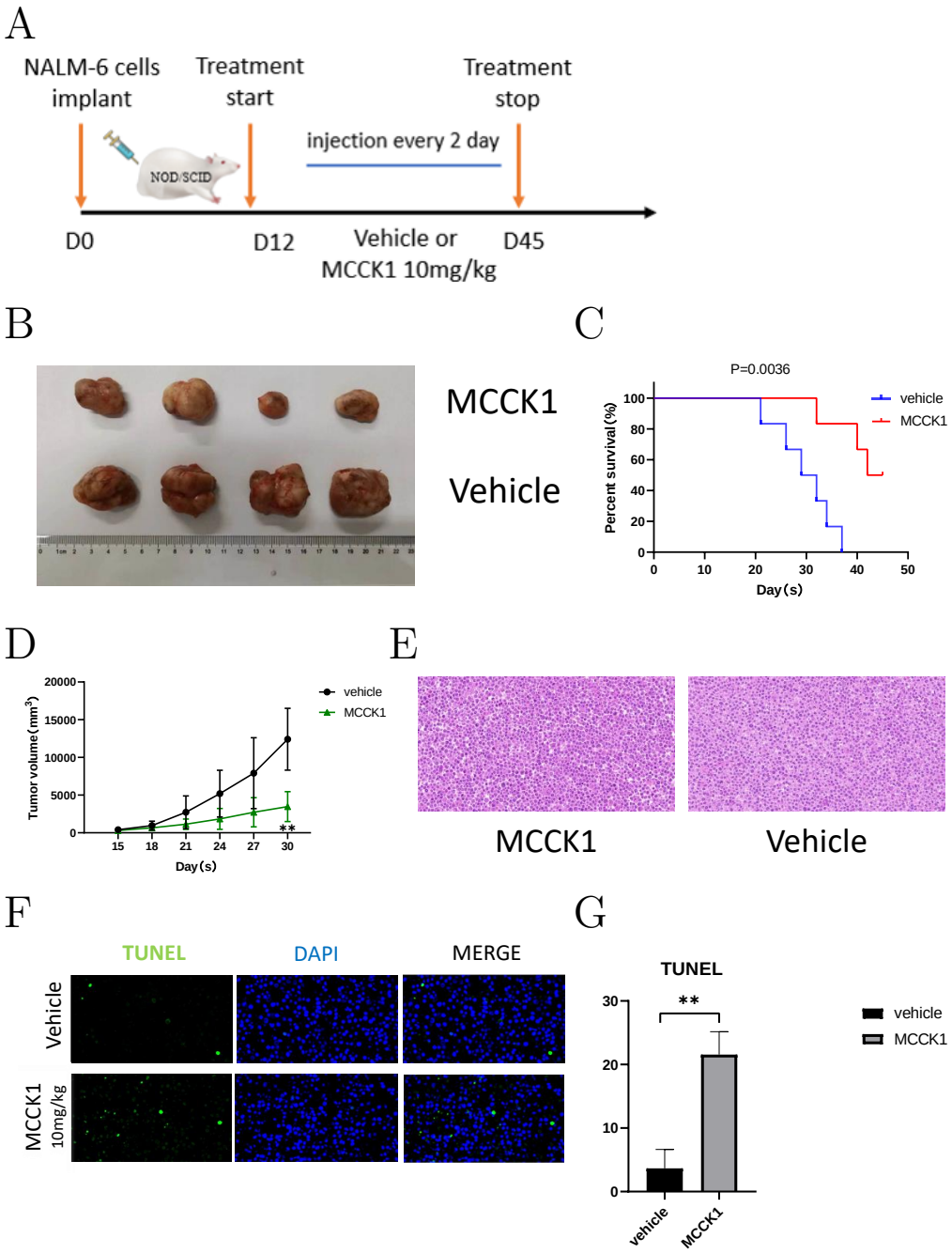

Figure 4. Investigations of MCCK1 on the growth of NALM-6 transplanted tumors in vivo. (A) NOD/SCID mice were implanted subcutaneously with NALM-6 cells and given either saline or MCCK1 via intraperitoneal injection every other day. (B) Images of subcutaneous xenografts from mice in the vehicle and MCCK1 groups (n = 8). (C) Tumor size was measured using calipers on days 15, 18, 21, 24, 27, and 30, with calculations made according to the "in vivo study" formula. Data are expressed as mean ± standard deviation; *, $p < 0.05$ compared to the vehicle group; **, $p < 0.01$ compared to the vehicle group. (D) The survival curve of tumor-bearing mice was plotted using the Kaplan-Meier method. (E) H&E staining of xenograft tumors in each group at 20× magnification. (F) Stratified images of TUNEL immunofluorescence at 40× magnification. (G) Comparison of apoptotic cell differences between the two groups using gray-scale analysis.

4. Discussion

B-ALL is considered a malignancy of hematopoietic cells that typically exhibits genetic aberrations. Many cases of B-ALL have recurrent chromosomal abnormalities, including balanced chromosomal translocation [29]. 20% of patients with B-ALL develop drug resistance during treatment. Low remission rates and high recurrence rates are responsible for the high mortality rate of the disease [30]. Therefore, unearthing novel therapeutic objectives and successful medications is a paramount and long-term mission for B-ALL treatment.

IKBKE is a crucial serine/threonine protein kinase that is involved in regulating inflammatory responses, immune cell activation, proliferation, and metabolic disorders [31]. Additionally, it plays a significant role in the development and progression of numerous solid tumors [32]. The overexpression of IKBKE has been linked to the growth of cancerous cells, migration, infiltration, and resistance to chemotherapy. Therefore, IKBKE has been demonstrated to foster development, multiplication, infiltration, and medication resistance in multiple malignancies [33–35]. The real-time PCR technique was employed to assess IKBKE kinase expression in B-ALL in this investigation. The expression of IKBKE kinase was more prominent in B-ALL patients as opposed to healthy individuals. It was found in past research that when MCCK1 restrained IKBKE, it caused the growth of cancer cells with IKBKE irregularities to cease and become apoptotic. Notably, previous studies have demonstrated that MCCK1 is a targeted inhibitor of IKBKE, specifically halting IKBKE's increase in human cancer cells in nude mice. However, it does not impact tumor growth in cancer cells lacking elevated levels of IKBKE [36, 37]. In line with previous findings, the current study discovered that MCCK1, a small-molecule inhibitor of IKBKE kinase, effectively suppressed the growth of NALM-6 and RS4:11 B-ALL cell lines, indicating its potential as a cytotoxic agent against these cancerous cells. Additionally, this study explored the drug's impact on apoptosis and cell cycle progression. A study found that the tumor cell cycle was blocked in the G0/G1 phase after treatment with an IKBKE inhibitor [38]. Consistent with these results, the study's findings revealed that MCCK1 triggers apoptosis and inhibits cell division during the G0/G1 phase. These results suggest that MCCK1 can reduce the growth of B-ALL cells by inducing apoptosis and halting cell cycle progression. The in vitro studies mentioned above demonstrated that MCCK1 inhibited the proliferation of B-ALL cells and promoted apoptosis. To further explore the anti-tumor effects of MCCK1, we created a NOD/SCID mouse model by injecting B-ALL cells subcutaneously. The NOD/SCID mouse model, a type of immune-science mouse model, is an excellent choice for conducting in vivo experiments on hematologic malignancies, as it displays a wide variety of immunological deficiencies [39]. Currently, subcutaneous injections are commonly used to generate hematologic tumors [40]. In vivo research has demonstrated that MCCK1 can suppress tumor expansion and induce apoptosis, which has confirmed its anti-tumor efficacy in B-ALL. Previous studies have shown that IKBKE does not directly activate the NF-kB pathway when interferon gene-stimulating factor (STING) is activated but drives the NF-kB pathway through its redundant interactions with TBK1 [41, 42], thereby affecting apoptosis [43]. Furthermore, IKBKE interacts with numerous proteins and is instrumental in controlling a multitude of signals. Up-regulation of IKBKE may lead to translocation of the GLI1 core and promote activation of AKT signaling after mTOR inhibition, thereby participating in cellular regulation [44]. More research is required to identify the signaling and associated regulatory elements involved in IKBKE in tumor cells since the role of IKBKE in the regulation of tumor cell signaling was neglected in this work. It is also known

that tumor cell resistance is closely linked to relapse in B-ALL disease. To continue this study, cell resistance experiments can be done with this drug compared to other chemotherapeutic agents.

In future work, our study could explore the integration of machine learning techniques in drug discovery efforts targeting B-ALL. Leveraging machine learning algorithms, such as molecular docking simulations and quantitative structure-activity relationship (QSAR) models, researchers could screen large libraries of compounds to identify potential inhibitors [45] of the IKBKE kinase, similar to MCCK1. These algorithms can efficiently analyze molecular structures and predict the binding affinity and biological activity of compounds against specific targets [46, 47], thereby accelerating the identification of novel therapeutic agents for B-ALL. Additionally, machine learning approaches can aid in the prediction of potential off-target effects and toxicity profiles [48], facilitating the selection of lead compounds with favorable pharmacological properties [49, 50]. By harnessing the predictive power of machine learning in drug discovery, future research endeavors could expedite the development of targeted therapies for B-ALL, ultimately improving patient outcomes.

5. Conclusions

In conclusion, B-ALL patients exhibit an excessive expression of MCCK1. MCCK1, an inhibitor of IKBKE, was observed to cause a substantial decrease in the growth of B-ALL cells in vitro through the initiation of apoptosis and a halt in the G0/G1 phase. MCCK1 decreased the proliferation of tumor cells in a living organism through toxic effects. This research shows that IKBKE not only inhibits proliferation and division of B-ALL cells in vitro but also inhibits B-ALL cell viability and induces apoptosis in vivo. Based on these results, IKBKE is a promising target for B-ALL therapy, and further research on innovative therapies for B-ALL patients is expected to be conducted.

Use of AI tools declaration

The authors declare they have not used Artificial Intelligence (AI) tools in the creation of this article.

Acknowledgments

This work was supported by the National Natural Science Foundation of China (No. 81960032, 82170168 and 82260728).

Conflict of interest

The authors declare there is no conflict of interest.

References

1. I. Aldoss, A. S. Stein, Advances in adult acute lymphoblastic leukemia therapy, *Leuk. Lymphoma*, **59** (2017), 1033–1050. http://dx.doi.org/10.1080/10428194.2017.1354372

2. Y. Jin, Z. Lu, K. Ding, J. Li, X. Du, C. Chen, et al., Antineoplastic mechanisms of niclosamide in acute myelogenous leukemia stem cells: Inactivation of the NF-κB pathway and generation of reactive oxygen species, *Cancer Res.*, **70** (2010), 2516–2527. http://dx.doi.org/10.1158/0008-5472.CAN-09-3950
3. S. Thota, A. Advani, Inotuzumab ozogamicin in relapsed B-cell acute lymphoblastic leukemia, *Eur. J. Haematol.*, **98** (2017), 425–434. http://dx.doi.org/10.1111/ejh.12862
4. N. Gokbuget, H. Dombret, J. M. Ribera, A. K. Fielding, A. Advani, R. Bassan, et al., International reference analysis of outcomes in adults with b-precursor ph-negative relapsed/refractory acute lymphoblastic leukemia, *Haematologica*, **101** (2016), 1524–1533. http://dx.doi.org/10.3324/haematol.2016.144311
5. D. Liu, J. Zhao, Y. Song, X. Luo, T. Yang, Clinical trial update on bispecific antibodies, antibody-drug conjugates, and antibody-containing regimens for acute lymphoblastic leukemia, *J. Hematol. Oncol.*, **12** (2019), 1–13. http://dx.doi.org/10.1186/s13045-019-0703-z
6. W. Liu, J. Ma, J. Chen, B. Huang, F. Liu, L. Li, et al., A novel TBK1/IKKϵ is involved in immune response and interacts with MyD88 and MAVS in the scallop Chlamys farreri, *Front. Immunol.*, **13** (2023), 1091419. http://dx.doi.org/10.3389/fimmu.2022.1091419
7. J. N. Brudno, J. N. Kochenderfer, Recent advances in CAR T-cell toxicity: Mechanisms, manifestations and management, *Blood Rev.*, **34** (2019), 45–55. http://dx.doi.org/10.1016/j.blre.2018.11.002
8. C. Bailly, The potential value of amlexanox in the treatment of cancer: Molecular targets and therapeutic perspectives, *Biochem. Pharmacol.*, **197** (2022), 114895. http://dx.doi.org/10.1016/j.bcp.2021.114895
9. D. A. Berry, S. Zhou, H. Higley, L. Mukundan, S. Fu, G. H. Reaman, et al., Association of minimal residual disease with clinical outcome in pediatric and adult acute lymphoblastic leukemia: A meta-analysis, *JAMA Oncol.*, **3** (2017), e170580. http://dx.doi.org/10.1001/jamaoncol.2017.0580
10. Q. A. Xiao, Q. He, L. Li, Y. Song, Y. R. Chen, J. Zeng, et al., Role of IKKε in the metabolic diseases: Physiology, pathophysiology, and pharmacology, *Front. Pharmacol.*, **13** (2022), 888588. http://dx.doi.org/10.3389/fphar.2022.888588
11. T. Liu, X. Gao, Y. Xin, Identification of an IKBKE inhibitor with antitumor activity in cancer cells overexpressing IKBKE, *Cytokine*, **116** (2019), 78–87. http://dx.doi.org/10.1016/j.cyto.2019.01.005
12. T. H. Tran, S. P. Hunger, The genomic landscape of pediatric acute lymphoblastic leukemia and precision medicine opportunities, *Semin. Cancer Biol.*, **84** (2022), 144–152. http://dx.doi.org/10.1016/j.semcancer.2020.10.013
13. J. P. Guo, S. K. Shu, L. He, Y. C. Lee, P. A. Kruk, S. Grenman, et al., Deregulation of IKBKE is associated with tumor progression, poor prognosis, and cisplatin resistance in ovarian cancer, *Am. J. Pathol.*, **175** (2009), 324–333. http://dx.doi.org/10.2353/ajpath.2009.080767
14. T. S. Elton, H. Selemon, S. M. Elton, N. L. Parinandi, Regulation of the MIR155 host gene in physiological and pathological processes, *Gene*, **532** (2013), 1–12. http://dx.doi.org/10.1016/j.gene.2012.12.009

15. H. J. Maier, T. G. Schips, A. Wietelmann, M. Krüger, C. Brunner, M. Sauter, et al., Cardiomyocyte-specific IκB kinase (IKK)/NF-κB activation induces reversible inflammatory cardiomyopathy and heart failure, *Proc. Natl. Acad. Sci.*, **109** (2012), 11794–11799. http://dx.doi.org/10.1073/pnas.1116584109

16. M. Yin, X. Wang, J. Lu, Advances in IKBKE as a potential target for cancer therapy, *Cancer Med.*, **9** (2019), 247–258. http://dx.doi.org/10.1002/cam4.2678

17. S. I. Göktuna, IKBKE-driven TPL2 and MEK1 phosphorylations sustain constitutive ERK1/2 activation in tumor cells, *EXCLI J.*, **21** (2022), 436. https://www.excli.de/index.php/excli/article/view/4578

18. R. T. Bishop, S. Marino, D. de Ridder, R. J. Allen, D. V. Lefley, A. H. Sims, et al., Pharmacological inhibition of the IKKε/TBK-1 axis potentiates the anti-tumour and anti-metastatic effects of docetaxel in mouse models of breast cancer, *Cancer Lett.*, **450** (2019), 76–87. http://dx.doi.org/10.1016/j.canlet.2019.02.032

19. M. M. Uddin, B. Gaire, B. Deza, I. Vancurova, *Interleukin-8-Induced Invasion Assay in Triple-Negative Breast Cancer Cells*, Springer US, 2020. http://dx.doi.org/10.1007/978-1-0716-0247-8_9

20. M. Leonardi, E. Perna, S. Tronnolone, D. Colecchia, M. Chiariello, Activated kinase screening identifies the IKBKE oncogene as a positive regulator of autophagy, *Autophagy*, **15** (2018), 312–326. http://dx.doi.org/10.1080/15548627.2018.1517855

21. J. Guo, D. Kim, J. Gao, C. Kurtyka, H. Chen, C. Yu, et al., IKBKE is induced by STAT3 and tobacco carcinogen and determines chemosensitivity in non-small cell lung cancer, *Oncogene*, **32** (2012), 151–159. http://dx.doi.org/10.1038/onc.2012.39

22. K. R. Balka, C. Louis, T. L. Saunders, A. M. Smith, D. J. Calleja, D. B. D'Silva, et al., TBK1 and IKKε act redundantly to mediate STING-induced NF-κB responses in myeloid cells, *Cell Rep.*, **31** (2020), 107492. http://dx.doi.org/10.1016/j.celrep.2020.03.056

23. S. Liu, A. E. Marneth, G. Alexe, S. R. Walker, H. I. Gandler, D. Q. Ye, et al., The kinases IKBKE and TBK1 regulate MYC-dependent survival pathways through YB-1 in AML and are targets for therapy, *Blood Adv.*, **2** (2018), 3428–3442. http://dx.doi.org/10.1182/bloodadvances.2018016733

24. J. Chen, X. Li, H. Liu, D. Zhong, K. Yin, Y. Li, et al., Bone marrow stromal cell-derived exosomal circular RNA improves diabetic foot ulcer wound healing by activating the nuclear factor erythroid 2-related factor 2 pathway and inhibiting ferroptosis, *Diabet. Med.*, **40** (2023), e15031. http://dx.doi.org/10.1111/dme.15031

25. S. Okada, K. Vaeteewoottacharn, R. Kariya, Application of highly immunocompromised mice for the establishment of patient-derived xenograft (PDX) models, *Cells*, **8** (2019), 889. http://dx.doi.org/10.3390/cells8080889

26. A. Riemann, S. Reime, O. Thews, Acidic extracellular environment affects miRNA expression in tumors in vitro and in vivo, *Int. J. Cancer*, **144** (2018), 1609–1618. http://dx.doi.org/10.1002/ijc.31790

27. A. Bainbridge, S. Walker, J. Smith, K. Patterson, A. Dutt, Y. M. Ng, et al., IKBKE activity enhances AR levels in advanced prostate cancer via modulation of the Hippo pathway, *Nucleic Acids Res.*, **48** (2020), 5366–5382. http://dx.doi.org/10.1093/nar/gkaa271

28. Y. Liu, J. Lu, Z. Zhang, L. Zhu, S. Dong, G. Guo, et al., Amlexanox, a selective inhibitor of IKBKE, generates anti-tumoral effects by disrupting the Hippo pathway in human glioblastoma cell lines, *Cell Death Dis.*, **8** (2017), e3022–e3022. http://dx.doi.org/10.1038/cddis.2017.396

29. A. S. Duffield, C. G. Mullighan, M. J. Borowitz, International consensus classification of acute lymphoblastic leukemia/lymphoma, *Virchows Arch.*, **482** (2022), 11–26. http://dx.doi.org/10.1007/s00428-022-03448-8

30. H. M. Kantarjian, D. J. DeAngelo, M. Stelljes, M. Liedtke, W. Stock, N. Gökbuget, et al., Inotuzumab ozogamicin versus standard of care in relapsed or refractory acute lymphoblastic leukemia: Final report and long-term survival follow-up from the randomized, phase 3 INOVATE study, *Cancer*, **125** (2019), 2474–2487. http://dx.doi.org/10.1002/cncr.32116

31. C. Taştan, D. D. Kançağı, R. D. Turan, B. Yurtsever, D. undefinedakırsoy, S. Abanuz, et al., Preclinical assessment of efficacy and safety analysis of CAR-T cells (ISIKOK-19) targeting CD19-expressing b-cells for the first turkish academic clinical trial with relapsed/refractory ALL and NHL patients, *Turk. J. Haematol.*, **37** (2020), 234–247. http://dx.doi.org/10.4274/tjh.galenos.2020.2020.0070

32. S. Challa, J. P. Guo, X. Ding, C. X. Xu, Y. Li, D. Kim, et al., IKBKE is a substrate of EGFR and a therapeutic target in non-small cell lung cancer with activating mutations of EGFR, *Cancer Res.*, **76** (2016), 4418–4429. http://dx.doi.org/10.1158/0008-5472.CAN-16-0069

33. J. Cui, C. Wei, L. Deng, X. Kuang, Z. Zhang, C. Pierides, et al., MicroRNA-143 increases cell apoptosis in myelodysplastic syndrome through the Fas/FasL pathway both in-vitro and in-vivo, *Int. J. Oncol.*, **53** (2018), 2191–2199. http://dx.doi.org/10.3892/ijo.2018.4534

34. M. C. J. Bosman, J. J. Schuringa, W. J. Quax, E. Vellenga, Bortezomib sensitivity of acute myeloid leukemia CD34+ cells can be enhanced by targeting the persisting activity of NF-κB and the accumulation of MCL-1, *Exp. Hematol.*, **41** (2013), 530–538. http://dx.doi.org/10.1016/j.exphem.2013.02.002

35. D. Bauer, E. Mazzio, K. F. Soliman, Whole transcriptomic analysis of apigenin on TNFα immuno-activated MDA-MB-231 breast cancer cells, *Cancer Genom, Proteomics*, **16** (2019), 421–431. http://dx.doi.org/10.21873/cgp.20146

36. K. P. Seastedt, N. Pruett, C. D. Hoang, Mouse models for mesothelioma drug discovery and development, *Expert Opin. Drug Discov.*, **16** (2020), 697–708. http://dx.doi.org/10.1080/17460441.2021.1867530

37. T. Liu, A. Li, Y. Xu, Y. Xin, MCCK1 enhances the anticancer effect of temozolomide in attenuating the invasion, migration and epithelial-mesenchymal transition of glioblastoma cells in vitro and in vivo, *Cancer Med.*, **8** (2019), 751–760. http://dx.doi.org/10.1002/cam4.1951

38. J. S. Boehm, J. J. Zhao, J. Yao, S. Y. Kim, R. Firestein, I. F. Dunn, et al., Integrative genomic approaches identify IKBKE as a breast cancer oncogene, *Cell*, **129** (2007), 1065–1079. http://dx.doi.org/10.1016/j.cell.2007.03.052

39. R. J. Oldham, C. I. Mockridge, S. James, P. J. Duriez, H. T. C. Chan, K. L. Cox, et al., FcγRII (CD32) modulates antibody clearance in NOD SCID mice leading to impaired antibody-mediated tumor cell deletion, *J. Immunother. Cancer*, **8** (2020), e000619. http://dx.doi.org/10.1136/jitc-2020-000619

40. Y. W. Lin, Z. M. Beharry, E. G. Hill, J. H. Song, W. Wang, Z. Xia, et al., A small molecule inhibitor of Pim protein kinases blocks the growth of precursor T-cell lymphoblastic leukemia/lymphoma, *Blood*, **115** (2010), 824–833. http://dx.doi.org/10.1182/blood-2009-07-233445

41. J. Hwee, R. Sutradhar, J. C. Kwong, L. Sung, S. Cheng, J. D. Pole, Infections and the development of childhood acute lymphoblastic leukemia: a population-based study, *Eur. J. Cancer Prev.*, **29** (2020), 538–545. http://dx.doi.org/10.1097/CEJ.0000000000000564

42. M. W. Lato, A. Przysucha, S. Grosman, J. Zawitkowska, M. Lejman, The new therapeutic strategies in pediatric T-cell acute lymphoblastic leukemia, *Int. J. Mol. Sci.*, **22** (2021), 4502. http://dx.doi.org/10.3390/ijms22094502

43. N. Safari-Alighiarloo, M. Taghizadeh, S. M. Tabatabaei, S. Namaki, M. Rezaei-Tavirani, Identification of common key genes and pathways between type 1 diabetes and multiple sclerosis using transcriptome and interactome analysis, *Endocrine*, **68** (2020), 81–92. http://dx.doi.org/10.1007/s12020-019-02181-8

44. W. Xie, S. Tian, J. Yang, S. Cai, S. Jin, T. Zhou, et al., OTUD7B deubiquitinates SQSTM1/p62 and promotes IRF3 degradation to regulate antiviral immunity, *Autophagy*, **18** (2022), 2288–2302. http://dx.doi.org/10.1080/15548627.2022.2026098

45. J. Zhao, Y. Liu, L. Zhu, J. Li, Y. Liu, J. Luo, et al., Tumor cell membrane-coated continuous electrochemical sensor for GLUT1 inhibitor screening, *J. Pharm. Anal.*, **13** (2023), 673–682. http://dx.doi.org/10.1016/j.jpha.2023.04.015

46. T. H. Nguyen-Vo, Q. H. Trinh, L. Nguyen, P. U. Nguyen-Hoang, T. N. Nguyen, D. T. Nguyen, et al., iCYP-MFE: Identifying human cytochrome P450 inhibitors using multitask learning and molecular fingerprint-embedded encoding, *J. Chem. Inf. Model.*, **62** (2021), 5059–5068. http://dx.doi.org/10.1021/acs.jcim.1c00628

47. Y. Zhu, R. Huang, Z. Wu, S. Song, L. Cheng, R. Zhu, Deep learning-based predictive identification of neural stem cell differentiation, *Nat. Commun.*, **12** (2021), 2614. http://dx.doi.org/10.1038/s41467-021-22758-0

48. T. H. Nguyen-Vo, L. Nguyen, N. Do, P. H. Le, T. N. Nguyen, B. P. Nguyen, et al., Predicting drug-induced liver injury using convolutional neural network and molecular fingerprint-embedded features, *ACS Omega*, **5** (2020), 25432–25439. http://dx.doi.org/10.1021/acsomega.0c03866

49. L. Nguyen, T. H. Nguyen Vo, Q. H. Trinh, B. H. Nguyen, P. U. Nguyen-Hoang, L. Le, et al., iANP-EC: Identifying anticancer natural products using ensemble learning incorporated with evolutionary computation, *J. Chem. Inf. Model.*, **62** (2022), 5080–5089. http://dx.doi.org/10.1021/acs.jcim.1c00920

50. T. H. Nguyen-Vo, Q. H. Trinh, L. Nguyen, T. T. T. Do, M. C. H. Chua, B. P. Nguyen, Predicting antimalarial activity in natural products using pretrained bidirectional encoder representations from transformers, *J. Chem. Inf. Model.*, **62** (2021), 5050–5058. http://dx.doi.org/10.1021/acs.jcim.1c00584

AIMS Press